Electronic Supplementary Information for:
Circular dichroism in non-chiral metal halide perovskites

Peter C. Sercel [1,a)], Zeev Valy Vardeny [2], and Alexander L. Efros [3]

[1] *Department of Applied Physics and Materials Science, California Institute of Technology, Pasadena, California 91125, USA; Electronic mail: psercel@caltech.edu*

[a)] *Also at Center for Hybrid Organic Inorganic Semiconductors for Energy, 15013 Denver West Parkway, Golden, CO 80401, USA*

[2] *Department of Physics and Astronomy, University of Utah, Salt Lake City, UT 84112, USA*

[3] *Center for Computational Materials Science, U. S. Naval Research Laboratory, Washington DC 20375 USA*

CONTENTS

S1. MATRIX REPRESENTATION OF THE RASHBA HAMILTONIAN FOR CENTER OF MASS MOTION OF EXCITONS

As we showed in the main text, for a 2D perovskite system with inversion symmetry breaking in the $\hat{z}$ direction and with Rashba splitting in the conduction band, the Rashba Hamiltonian $\hat{H}_{R,\mathrm{COM}}$ for an exciton with wave vector $\boldsymbol{K} = K_x\hat{x} + K_y\hat{y}$ in the plane reduces

to,

$$\hat{H}_{R,\text{COM}}(\boldsymbol{K}) = \frac{m_e}{M}\left(\alpha_{xy}K_y J_x - \alpha_{yx}K_x J_y\right) \ . \tag{S1}$$

Maintaining the general notation used in Eq.S1, it is convenient to represent $\hat{H}_{R,\text{COM}}(\boldsymbol{K})$ in Eq.(S1) in matrix form in a basis of the four electron and hole Bloch function products, $|u_{j_e=1/2}\rangle|u_{j_h=1/2}\rangle$, $|u_{j_e=1/2}\rangle|u_{j_h=-1/2}\rangle$, $|u_{j_e=-1/2}\rangle|u_{j_h=1/2}\rangle$ and $|u_{j_e=-1/2}\rangle|u_{j_h=-1/2}\rangle$. Using this pair ("P") basis gives the following matrix representation:

$$\hat{H}^{\text{P}}_{R,COM}(\boldsymbol{K}) = \frac{m_e}{M}\begin{pmatrix} 0 & 0 & \alpha_{xy}K_y + i\alpha_{yx}K_x & 0 \\ 0 & 0 & 0 & \alpha_{xy}K_y + i\alpha_{yx}K_x \\ \alpha^e_{xy}K_y - i\alpha_{yx}K_x & 0 & 0 & 0 \\ 0 & \alpha_{xy}K_y - i\alpha_{yx}K_x & 0 & 0 \end{pmatrix} \tag{S2}$$

We can easily transform this Hamiltonian into a basis of exciton eigenstates of total angular momentum, $|F, F_z\rangle$, taken in the order, $|0,0\rangle$, $|1,1\rangle$, $|1,0\rangle$, $|1,-1\rangle$. This is done using the transformation $\hat{H}^{F,F_z} = \hat{m}^{-1}_{P,F}\hat{H}^P(\boldsymbol{K})\hat{m}_{P,F}$, where

$$\hat{m}_{P,F} = \begin{pmatrix} 0 & 1 & 0 & 0 \\ -\frac{1}{\sqrt{2}} & 0 & \frac{1}{\sqrt{2}} & 0 \\ \frac{1}{\sqrt{2}} & 0 & \frac{1}{\sqrt{2}} & 0 \\ 0 & 0 & 0 & 1 \end{pmatrix} \ . \tag{S3}$$

The result is,

$$\hat{H}^{F,F_z}_{R,\text{COM}}(\boldsymbol{K}) = \frac{m_e}{M}\begin{pmatrix} 0 & \frac{\alpha_{xy}K_y - i\alpha_{yx}K_x}{\sqrt{2}} & 0 & -\frac{\alpha_{xy}K_y + i\alpha_{yx}K_x}{\sqrt{2}} \\ \frac{\alpha_{xy}K_y + i\alpha_{yx}K_x)}{\sqrt{2}} & 0 & \frac{\alpha_{xy}K_y + i\alpha_{yx}K_x}{\sqrt{2}} & 0 \\ 0 & \frac{\alpha_{xy}K_y - i\alpha_{yx}K_x}{\sqrt{2}} & 0 & \frac{\alpha_{xy}K_y + i\alpha^e_{yx}K_x}{\sqrt{2}} \\ \frac{-\alpha_{xy}K_y + i\alpha_{yx}K_x)}{\sqrt{2}} & 0 & \frac{\alpha_{xy}K_y - i\alpha^e_{yx}K_x}{\sqrt{2}} & 0 \end{pmatrix} \tag{S4}$$

To study polarization properties it is most convenient to transform into a basis of exciton states whose dipoles are oriented along the x, y, z directions. We will call the D, X, Y, Z basis, or the $\mathcal{O}$ basis for short, the basis of exciton states $|D\rangle$, $|X\rangle$, $|Y\rangle$, $|Z\rangle$, whose dipoles are oriented along the X, Y, and Z directions, and the dark D exciton state. The unitary transformation from the basis of total exciton angular momentum to the $\mathcal{O}$ basis is,

$$\hat{H}^{D,X,Y,Z}_{R,\text{COM}}(\boldsymbol{K}) = \tilde{m}^{-1}_{FO}\hat{H}^{F,F_z}_{R,\text{COM}}(\boldsymbol{K})\tilde{m}_{FO} \tag{S5}$$

where the transformation matrix, $\tilde{m}_{FO} = \langle F, F_z | \mathcal{O} \rangle$ is given by,

$$\tilde{m}_{FO} = \begin{pmatrix} 1 & 0 & 0 & 0 \\ 0 & -\frac{1}{\sqrt{2}} & \frac{i}{\sqrt{2}} & 0 \\ 0 & 0 & 0 & 1 \\ 0 & \frac{1}{\sqrt{2}} & \frac{i}{\sqrt{2}} & 0 \end{pmatrix} \quad \text{(S6)}$$

The Hamiltonian is represented in the $\mathcal{O}$ or D, X, Y, Z basis by the matrix,

$$\hat{H}_{R,\text{COM}}^{D,X,Y,Z}(\boldsymbol{K}) = \frac{m_e}{M} \times \begin{pmatrix} 0 & -\alpha_{xy}K_y & \alpha_{yx}K_x & 0 \\ -\alpha_{xy}K_y & 0 & 0 & -i\alpha_{yx}K_x \\ \alpha_{yx}K_x & 0 & 0 & -i\alpha_{xy}K_y \\ 0 & i\alpha_{yx}K_x & i\alpha_{xy}K_y & 0 \end{pmatrix} \quad \text{(S7)}$$

A. Diagonalization of the exciton COM Hamiltonian and COM dispersion

Diagonalization of Eq. S7 shows that non-zero $\boldsymbol{K}$ splits the degeneracy of the 4 exciton states. Taking into account the exciton kinetic energy $\hbar^2 K^2/2M$ written in terms of total exciton mass $M = m_e + m_h$, and using $K = \sqrt{K_x^2 + K_y^2}$, the energy for any momentum direction is determined as a function of K_x, K_y by,

$$E_{COM}(K) = \frac{\hbar^2 K^2}{2M} \pm \frac{m_e}{M} \sqrt{\alpha_{yx}^2 K_x^2 + \alpha_{xy}^2 K_y^2} \ . \quad \text{(S8)}$$

The COM motion of free excitons described by Eq. (S8) has the "Lifshitz Trousers" dispersion, well known for 2D electrons in the presence of Rashba terms. From Eq. S8 we can find the exciton minimum energy along a given direction and estimate a wave vector K that is relevant to a thermalized exciton population at low temperature. In the absence of the exciton fine structure splitting at $K = 0$, and if $\alpha_{yx} = \pm\alpha_{xy}$, corresponding to the pure Rashba case, $\alpha_{xy} = \alpha$, or the pure Dresselhaus case, $\alpha_{xy} = \beta$ as discussed in the main text, the dispersion is *isotropic* in the K_x, K_y plane with the minimum of the dispersion at the radial wavenumber,

$$K_{min} = \frac{|\alpha_{xy}m_e|}{\hbar^2} \quad \text{(S9)}$$

The band dispersion for *electrons* reaches its minimum at the Rashba wave vector, $K_R^e = m_e\alpha^e/\hbar^2$. As a result the exciton COM dispersion minima also occurs at the Rashba wave

vector,

$$K_{min} = |K_R^e| \tag{S10}$$

In the general case that $\alpha_{yx} \neq \alpha_{xy}$ the dispersion is not isotropic and the energy contours in the K_x, K_y plane are warped with two-fold rotational symmetry.

A complete description of the exciton dispersion requires that we also include the exciton fine structure splitting due to electron-hole exchange. Neglecting the exchange splitting between the X and Y exciton states, which is small in comparison to the splitting between the Z exciton and the X, Y excitons in 2D perovskites,[S1] the fine structure Hamiltonian in the basis D, X, Y, Z can be written as,[S2,S3]

$$H_{fs} = \begin{pmatrix} E_d & 0 & 0 & 0 \\ 0 & E_t & 0 & 0 \\ 0 & 0 & E_t & 0 \\ 0 & 0 & 0 & E_z \end{pmatrix}. \tag{S11}$$

Thus the total Hamiltonian in the D, X, Y, Z basis is,

$$\hat{H}_{D,X,Y,Z}^{\mathrm{tot}}(\boldsymbol{K}) = \left[\mathcal{E}_{0,0} + \frac{\hbar^2(K_x^2 + K_y^2)}{2M} \right] \mathbb{I} +$$

$$\begin{pmatrix} E_d & -\alpha_{xy}K_y & \alpha_{yx}K_x & 0 \\ -\alpha_{xy}K_y & E_t & 0 & -i\alpha_{yx}K_x \\ \alpha_{yx}K_x & 0 & E_t & -i\alpha_{xy}K_y \\ 0 & i\alpha_{yx}K_x & i\alpha_{xy}K_y & E_z \end{pmatrix}. \tag{S12}$$

In this expression, $\mathbb{I}$ is the 4x4 unit matrix. Importantly the fine structure Hamiltonian in Eq. (S12) is not rotationally invariant in the general case. Nevertheless we can find solutions in several special cases. For the special case when $E_z = E_t$, and if $\alpha_{yx} = \pm\alpha_{xy}$ again corresponding to the pure Rashba case, $\alpha_{xy} = \alpha$, or the pure Dresselhaus case, $\alpha_{xy} = \beta$, the eigenvalues are,

$$E_{1,\pm1}(\boldsymbol{K}) = \mathcal{E}_{0,0} + \Delta + \frac{\hbar^2 K^2}{2M} \pm K\frac{m_e\alpha_{xy}}{M} ,$$

$$E_{1/2\pm1/2,0}(\boldsymbol{K}) = \mathcal{E}_{0,0} + \frac{\hbar^2 K^2}{2M} + \frac{\Delta}{2} \pm \frac{\sqrt{\Delta^2 M^2 + 4K^2(m_e\alpha_{xy})^2}}{2M} . \tag{S13}$$

Here, $\Delta \equiv E_t - E_d$ is the energy difference between the degenerate X and Y states and the dark exciton state. The subscripts on the energy in this expression refer to projection of the exciton angular momentum along a quantization axis that varies with $\boldsymbol{K}$, taken in the direction of the effective magnetic field at the given $\boldsymbol{K}$ point as described in the main text.

In the case of large dark- bright exciton splitting, Δ, the Rashba terms result in a small correction to the effective mass of the exciton center of mass motion for the bright and dark excitons with $F_{F_{z_B}} = 0$:

$$E_{1,0}(\boldsymbol{K}) = \mathcal{E}_{0,0} + \frac{\hbar^2 K^2}{2M} + \Delta + \frac{\hbar^2 K^2}{\Delta} \left(\frac{m_e \alpha_{xy}}{M} \right)^2 ,$$

$$E_{0,0}(\boldsymbol{K}) = \mathcal{E}_{0,0} + \frac{\hbar^2 K^2}{2M} - \frac{\hbar^2 K^2}{\Delta} \left(\frac{m_e \alpha_{xy}}{M} \right)^2 , \tag{S14}$$

In the more general case that the Z exciton state is split from the X and Y states, the triplet degeneracy at $\boldsymbol{K} = 0$ is lifted, resulting in a doublet with energy E_t and a singlet with energy $E_z \neq E_t$ at $\boldsymbol{K} = 0$. We set $\delta_z \equiv E_z - E_t$ and write the energies in the pure Rashba or pure Dresselhaus cases as,

$$E_{1,\pm 1}(\boldsymbol{K}) = \mathcal{E}_{0,0} + \Delta + \frac{\hbar^2 K^2}{2M} + \frac{\delta_z}{2} \pm \frac{\sqrt{\delta_z^2 M^2 + 4K^2 (m_e \alpha_{xy})^2}}{2M} ,$$

$$E_{1/2\pm 1/2,0}(\boldsymbol{K}) = \mathcal{E}_{0,0} + \frac{\hbar^2 K^2}{2M} + \frac{\Delta}{2} \pm \frac{\sqrt{\Delta^2 M^2 + 4K^2 (m_e \alpha_{xy})^2}}{2M} , \tag{S15}$$

The resulting dispersion and spin textures are plotted in Fig. S1. Parameters are the same as in Fig. 3 of the main text, but the bright triplet is assumed in Fig. S1 to be split by crystal field splitting, reflected in the triplet energies $E_x = E_y = E_t = 11.4$ meV, and $E_z = 1.2$ meV above the dark state at energy $E_D = 0$ meV.[S1,S4]

In the general case that $\alpha_{yx} \neq \alpha_{xy}$ where we have mixed Rashba and Dresselhaus character, we can also find analytical solutions for the energy. The general result is,

$$E_{1,\pm 1}(\boldsymbol{K}) = \mathcal{E}_{0,0} + \Delta + \frac{\hbar^2 K^2}{2M} + \frac{\delta_z}{2} \pm \frac{\sqrt{\delta_z^2 M^2 + 4m_e (K_x^2 \alpha_{yx}^2 + K_y^2 \alpha_{xy}^2)}}{2M} ,$$

$$E_{1/2\pm 1/2,0}(\boldsymbol{K}) = \mathcal{E}_{0,0} + \frac{\hbar^2 K^2}{2M} + \frac{\Delta}{2} \pm \frac{\sqrt{\Delta^2 M^2 + 4m_e (K_x^2 \alpha_{yx}^2 + K_y^2 \alpha_{xy}^2)}}{2M} , \tag{S16}$$

These solutions give energy contours that are not rotationally invariant about the z axis. In the most general case that the X and Y excitons are split are $\boldsymbol{K} = 0$, there is no closed form solution but the energies can be found using numerical diagonalization.

B. Effect of angular momentum textures: Transformation to rotated coordinate system

To understand the angular momentum textures of the excitons, it is useful to align the in-plane coordinate system with the direction of the wave vector $\boldsymbol{K}$. To do so, we represent $\boldsymbol{K} = K (\cos \phi \boldsymbol{n}_x + \sin \phi \boldsymbol{n}_y)$, where $K = \sqrt{k_x^2 + K_y^2}$, $\boldsymbol{n}_x$ and $\boldsymbol{n}_y$ are unit vectors along the
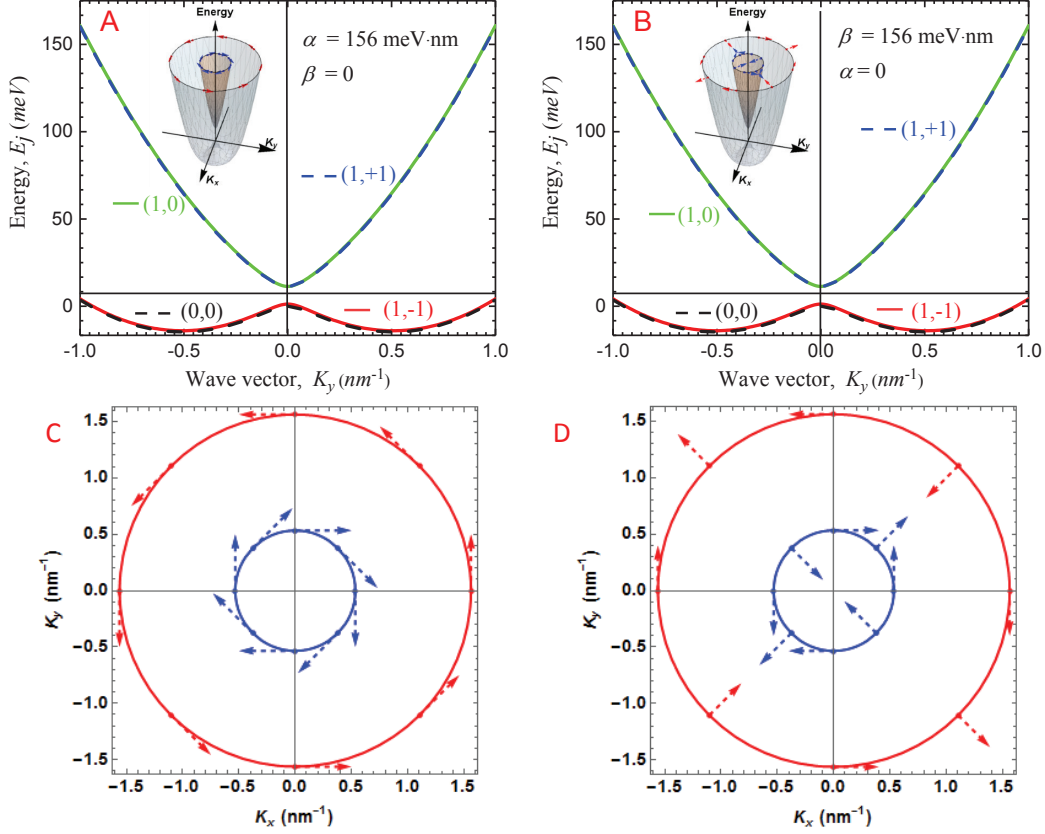
Figure S1. Exciton energies and angular momentum textures in 2D layered perovskite with inversion symmetry breaking along the $\hat{z}$ direction normal to the 2D plane, with crystal field splitting of the bright triplet. The bright triplet is assumed to be split by crystal field splitting, reflected in the triplet energies $E_x = E_y = E_t = 11.4$ meV, and $E_z = 1.2$ meV above the dark state at energy $E_D = 0$ meV.[S1,S4] Panels A and B show the energies calculated versus wave vector $\boldsymbol{K} = K_y \hat{y}$ for pure Rashba and pure 2D-Dresselhaus spin textures, respectively, with $\alpha = 156$ meV $\cdot$ nm, $\beta = 0$ in A, and $\alpha = 0$, $\beta = 156$ meV $\cdot$ nm in B. Electron and hole effective masses $m_e = m_h = 0.25 m_0$. The dispersion curves for each fine structure level in panels A and B are labelled according to (F, F_{z_B}), the exciton total angular momentum and its projection on an axis aligned to the effective magnetic field, see main text. The curves in A and B are identical reflecting symmetry under rotation about the $\hat{z}$ axis as evident in the insets of each figure, which show 3D plots of the energy surfaces in the K_x, K_y plane for the levels $(1, \pm 1)$. Panel C(D) shows the angular momentum textures for these two states along constant energy contours at $E = 70$ meV with parameters identical to panel A(B), respectively.

original x and y directions and angle ϕ is the angle between the new x' axis, (parallel to $\boldsymbol{K}$) and the original x axis in the 2D plane. The transition to this coordinate system leads to a unitary transformation of Hamiltonian $\hat{H}_{R,\text{COM}}^{D,X,Y,Z}(\boldsymbol{K})$ to a basis $|D\rangle$, $|X'\rangle$, $|Y'\rangle$, $|Z\rangle$ where the Hamiltonian can be represented as

$$\hat{H}_{R,\text{COM}}^{D,X',Y',Z}(K,\phi) = \frac{m_e}{M} K \times$$

$$\begin{pmatrix} 0 & -(\alpha_{xy}-\alpha_{yx})\sin\phi\cos\phi & \alpha_{xy}\sin^2\phi+\alpha_{yx}\cos^2\phi & 0 \\ -(\alpha_{xy}-\alpha_{yx})\sin\phi\cos\phi & 0 & 0 & -i(\alpha_{xy}\sin^2\phi+\alpha_{yx}\cos^2\phi) \\ \alpha_{xy}\sin^2\phi+\alpha_{yx}\cos^2\phi & 0 & 0 & -i(\alpha_{xy}-\alpha_{yx})\sin\phi\cos\phi \\ 0 & i(\alpha_{xy}\sin^2\phi+\alpha_{yx}\cos^2\phi) & i(\alpha_{xy}-\alpha_{yx})\sin\phi\cos\phi & 0 \end{pmatrix}$$

$$(S19)$$

The eigenfunctions of the Hamiltonian in Eq. (S19) are a mixture of the basis states $|D\rangle$, $|X'\rangle$, $|Y'\rangle$, and $|Z\rangle$. As a result each of the eigenstates of the Hamiltonian in Eq. (S19) has a well defined polarization which is described by the combination of three orthogonal linear polarized dipoles and the dipole forbidden state. The exact combination can be found by diagonalization of the total Hamiltonian

$$\hat{H}_{\text{tot}} = \hat{H}_{\text{INT}} + \hat{H}_{R,\text{COM}}^{D,X',Y',Z}(K,\phi) \tag{S20}$$

where $\hat{H}_{\text{INT}}$ describes the fine structure of the exciton connected with exciton internal motion at $K = 0$. The general solution of this problem cannot be put into in closed form but expressions for the pure Rashba and pure Dresselhaus cases are instructive.

In the pure Rashba case, corresponding to $\alpha_{yx} = \alpha_{xy} = \alpha$, Eq. S19 becomes,

$$\hat{H}_{R,\text{COM}}^{D,X',Y',Z}(K,\phi) = \frac{m_e}{M} K \begin{pmatrix} 0 & 0 & \alpha & 0 \\ 0 & 0 & 0 & -i\alpha \\ \alpha & 0 & 0 & 0 \\ 0 & i\alpha & 0 & 0 \end{pmatrix} \tag{S21}$$

Adding the center of mass and internal motion terms the total Hamiltonian is given for all values ϕ by,

$$\hat{H}_{D,X',Y',Z}^{\text{tot}}(\boldsymbol{K}) = \left(\mathcal{E}_{0,0} + \frac{\hbar^2 K^2}{2M}\right)\mathbb{I} + \begin{pmatrix} E_d & 0 & \frac{m_e}{M}K\alpha & 0 \\ 0 & E_t & 0 & -i\frac{m_e}{M}K\alpha \\ \frac{m_e}{M}K\alpha & 0 & E_t & 0 \\ 0 & i\frac{m_e}{M}K\alpha & 0 & E_z \end{pmatrix}, \tag{S22}$$

Recalling that the matrix is represented in the $\mathcal{O}'$ basis taken in the order D, X', Y', Z, this matrix clearly shows that the exciton eigenstates comprise two uncoupled pairs, one pair

comprising mixtures of the D and Y' basis states and the other comprising mixtures of the X' and Z basis states. Since the wave vector is in the X' direction, these state couple to light with linear dipoles (the x' components of the states cannot couple to light propagating in the x' direction). The energy eigenvalues are given by Eq. S15 using $\alpha_{xy} = \alpha$.

The pure Dresselhaus case, corresponding to $\alpha_{xy} = \beta = -\alpha_{yx}$, Eq. S19, is distinctly different. In this case the COM Hamiltonian becomes,

$$\hat{H}_{R,\mathrm{COM}}^{D,X',Y',Z}(K,\phi) = \frac{m_e}{M}K\begin{pmatrix} 0 & -\beta\sin 2\phi & -\beta\cos 2\phi & 0 \\ -\beta\sin 2\phi & 0 & 0 & i\beta\cos 2\phi \\ -\beta\cos 2\phi & 0 & 0 & -i\beta\sin 2\phi \\ 0 & -i\beta\cos 2\phi & i\beta\sin 2\phi & 0 \end{pmatrix}, \quad (S23)$$

This matrix can also be put into the form of two decoupled pairs, but the mixtures are more complex than in the pure Rashba case. It is simplest to analyze the matrix in two special cases. If $\phi = \pi/2n$ where n is an integer, that is, when $\boldsymbol{K}$ is along the x or y axes, then the matrix becomes identical to the one shown for the pure Rashba case and the eigenstates are the same. This reflects the fact that the direction of the effective magnetic field is the same for pure Rashba and Dresselhaus spin textures for $\boldsymbol{K}$ directed along the symmetry axes K_x and K_y, see Fig. 2 in the main text. On the other hand, when $\phi = \pi/4(2n+1)$ with n integer, then the matrix is distinct from that of the pure Rashba case:

$$\hat{H}_{R,\mathrm{COM}}^{D,X',Y',Z}\left(K,\phi = \frac{\pi(2n+1)}{4}\right) = (-1)^n\frac{m_e}{M}K\beta\begin{pmatrix} 0 & -1 & 0 & 0 \\ -1 & 0 & 0 & 0 \\ 0 & 0 & 0 & -i \\ 0 & 0 & i & 0 \end{pmatrix}. \quad (S24)$$

In this case it is clear that there are two decoupled pairs of states, one pair comprising mixtures of the D and X' basis states and the other comprising a superposition of the Y' and Z basis states. The later pair has a total angular momentum $F = 1$ with the projection of angular momentum in the direction of $\boldsymbol{K}$ of $F_{\hat{K}} = \pm 1$ and therefore has helicity. These states will couple preferentially to helical light with positive and negative helicity, respectively. To show this we add in the center of mass and internal motion terms to form the total Hamiltonian for $\phi = \pi/4$, that is, with $\boldsymbol{K}$ along the line $K_x = K_y$. In

this case the Hamiltonian is,

$$\hat{H}_{D,X',Y',Z}^{\mathrm{tot}}(K_x = K_y) = \left(\mathcal{E}_{0,0} + \frac{\hbar^2 K^2}{2M}\right)\mathbb{I} + \begin{pmatrix} E_d & -\frac{m_e}{M}K\beta & 0 & 0 \\ -\frac{m_e}{M}K\beta & E_t & 0 & 0 \\ 0 & 0 & E_t & -i\frac{m_e}{M}K\beta \\ 0 & 0 & i\frac{m_e}{M}K\beta & E_z \end{pmatrix}, \quad \text{(S25)}$$

The energy eigenvalues are again given by Eq. S15 using $\alpha_{xy} = \beta$.

S2. CD CALCULATION

A. Description of polarization and CD measurement geometry

In this study we calculate the magnitude of the CD signal of a 2D perovskite layer with orthorhombic symmetry C_{2v}. We consider the sample, depicted in Fig. S2, to be oriented in the x, y plane, with the 2D layers parallel to the top surface of the sample which is normal to the z direction. The sample has two-fold rotational symmetry about the z axis, with inversion symmetry broken along the z direction, and mirror symmetry through the x, z and y, z planes. The sample is assumed to have refractive index n_{mat} and to be illuminated from air at a polar incidence angle θ measured from the vertical, z, axis in a plane of incidence defined by azimuthal angle ϕ measured from the x axis according to Fig. S2. We consider the incident light to be circularly polarized with helicity ± 1, corresponding to angular momentum ± 1 along the $\boldsymbol{K}$ direction. For light with its wave vector $\boldsymbol{k}_{ph}$ directed in the positive $\hat{\boldsymbol{z}}$ direction the ± 1 polarizations vectors are,

$$\hat{e}_{\pm} = \frac{\hat{\boldsymbol{x}} \pm i\hat{\boldsymbol{y}}}{\sqrt{2}} \quad \text{(S26)}$$

These correspond to left $(+)$ and right $(-)$ circular polarization respectively.[S5] The vector potential of $\hat{e}_{\pm}$ helical light of amplitude A_0 propagating in the $\hat{\boldsymbol{z}}$ direction is therefore,

$$\boldsymbol{A}_{\pm,\boldsymbol{k}_{ph}=k_{ph}\hat{\boldsymbol{z}}} = A_0\hat{e}_{\pm} = A_0\frac{\hat{\boldsymbol{x}} \pm i\hat{\boldsymbol{y}}}{\sqrt{2}} \quad \text{(S27)}$$

The incident light wave vector shown in Fig. S2 is not propagating in the positive $\hat{\boldsymbol{z}}$ direction. To determine the vector potential we must rotate both the wavevector $\boldsymbol{k}_{ph}$ and the polarization vectors $\hat{e}_{\pm}$ into an orientation corresponding with the schematic. First consider light incident in the positive $\hat{\boldsymbol{z}}$ direction, $\boldsymbol{k}_{ph} = k_{ph}\hat{\boldsymbol{z}}$; we need to obtain $\boldsymbol{k}_{ph}$, and the polarization vectors $\hat{e}_{\pm}$ oriented as in the figure with polar angle θ towards the
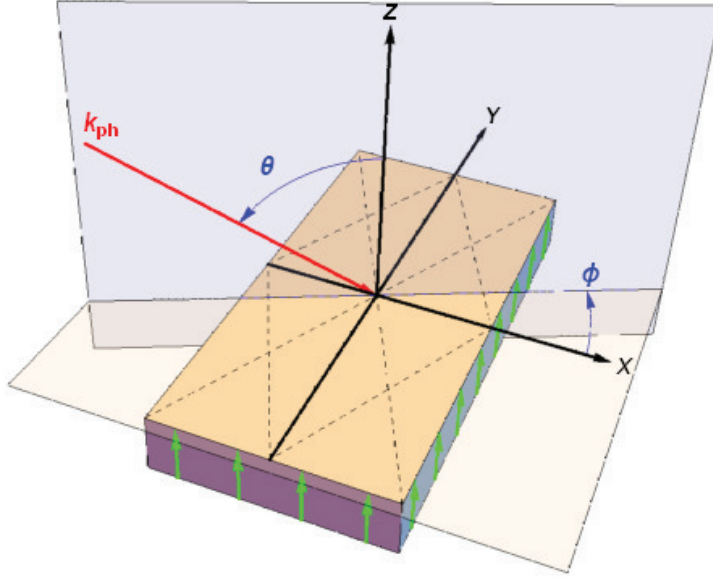
Figure S2.   Schematic of the sample and CD measurement geometry. Circularly polarized light with polarization $\hat{e}_\pm$ and wave vector $\boldsymbol{k}_{ph}$ is incident from air onto the sample, which has refractive index n_{mat}. The light is incident at polar angle θ measured from the layer normal, at azimuth angle ϕ measured from the x axis. The sample has 2D perovskite layers and orthorhombic symmetry. Layers are oriented in the x, y plane, parallel to the top surface of the sample which is normal to the inversion symmetry breaking direction along z. The sample has two-fold rotational symmetry about the z axis and mirror symmetry through the x, z and y, z planes.

negative $\hat{\boldsymbol{x}}$ direction and azimuth angle ϕ relative to the $\hat{\boldsymbol{x}}$ direction. This transformation is accomplished by first rotating about the $\hat{\boldsymbol{y}}$ direction by angle $\gamma = \pi - \theta_{inc}$ using $\boldsymbol{k}_{ph} = \tilde{R}_y(\gamma)k_{ph}\hat{\boldsymbol{z}}$ where the rotation is represented by the matrix,

$$\tilde{R}_y(\gamma) = \begin{pmatrix} \cos\gamma & 0 & +\sin\gamma \\ 0 & 1 & 0 \\ -\sin\gamma & 0 & \cos\gamma \end{pmatrix} \tag{S28}$$

Following this rotation the vectors are rotated about the positive $\hat{\boldsymbol{z}}$ direction using the rotation operator $\tilde{R}_z(\phi)$ represented by,

$$\tilde{R}_z(\phi) = \begin{pmatrix} \cos\phi & -\sin\phi & 0 \\ +\sin\phi & \cos\phi & 0 \\ 0 & 0 & 1 \end{pmatrix} \tag{S29}$$

An additional detail must be accounted for however: The angle of propagation of the light inside the perovskite layer, θ_{mat}, is related to the exterior angle of incidence θ by Snell's law,

$$\sin\theta = n_{\text{mat}}\sin\theta_{mat} \tag{S30}$$

Moreover the amplitude of the transmitted electric field is modified by the polarization-dependent Fresnel amplitude transmission coefficients. For light with its field vector polarized parallel versus perpendicular to the incidence plane these coefficients are given by,

$$t_\parallel(\theta, \theta_{mat}) = \frac{2\cos\theta}{\cos\theta_{mat} + n_{mat}\cos\theta} \tag{S31}$$

$$t_\perp(\theta, \theta_{mat}) = \frac{2\cos\theta}{\cos\theta + n_{mat}\cos\theta_{mat}} \ . \tag{S32}$$

The amplitude transmission coefficients are shown in Fig S3 calculated for light incident from air (refractive index 1) into a perovskite sample with a refractive index $n_{mat} = 5$. At large incidence angles θ the degree of circular polarization of the transmitted light is reduced due to the fact that the field component perpendicular to the plane of incidence has lower transmission that the field component parallel to the plane of incidence. This effect needs to be taken into account for a CD measurement where the incident light is set to be perfectly circular in the laboratory before impinging on the sample. The effect is that, for light propagating as shown in Fig. S2 the transmitted light has wave vector $\boldsymbol{k}_{ph,mat}$, with magnitude $k_{ph,mat} = 2\pi n_{mat}/\lambda_0$ and direction defined by azimuthal angle ϕ, polar angle θ_{mat} from the vertical, set by Snell's law. It has amplitude,

$$\boldsymbol{A}_\pm(\theta_{mat}, \phi) = A_0\hat{\boldsymbol{e}}_\pm(\theta_{mat}, \phi) \tag{S33}$$

where we have defined,

$$\hat{\boldsymbol{e}}_\pm(\theta_{mat}, \phi) \equiv \frac{1}{\sqrt{2}}\left[t_\parallel(\theta_{mat})\hat{\boldsymbol{e}}_\parallel(\theta_{mat}, \phi) \pm it_\perp(\theta_{mat})\hat{\boldsymbol{e}}_\perp(\theta_{mat}, \phi)\right] \ . \tag{S34}$$

Here, the vectors $\hat{\boldsymbol{e}}_\parallel$ and $\hat{\boldsymbol{e}}_\perp$ set the two orthogonal polarization directions normal to the direction of propagation $\boldsymbol{k}_{ph,mat}$ in the material, parallel and perpendicular to the plane of incidence, respectively. These are found by starting from Eq. S26 for light propagating in the positive $\hat{\boldsymbol{z}}$ direction and rotating them using the rotation matrices, Eqs. S28-S29:

$$\hat{\boldsymbol{e}}_\parallel(\theta_{mat}, \phi) = \tilde{R}_z(\phi)\tilde{R}_y(\pi - \theta_{mat})\hat{\boldsymbol{x}} \tag{S35}$$

$$\hat{\boldsymbol{e}}_\perp(\theta_{mat}, \phi) = \tilde{R}_z(\phi)\tilde{R}_y(\pi - \theta_{mat})\hat{\boldsymbol{y}} \tag{S36}$$

For reference, the result for light incident in the x, z plane ($\phi = 0$) is,

$$\hat{e}_{\parallel}(\theta_{mat}, 0) = -\frac{1}{\sqrt{2}} \left(\cos \theta_{mat} \hat{x} + \sin \theta_{mat} \hat{z} \right) \tag{S37}$$

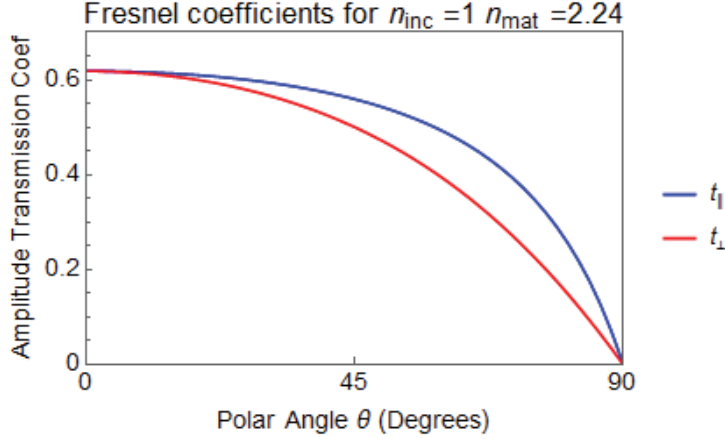$$\hat{e}_{\perp}(\theta_{mat}, 0) = \frac{1}{\sqrt{2}} \hat{y} \tag{S38}$$

Figure S3.   Amplitude transmission coefficients $t_{\parallel}$ and $t_{\perp}$ for light with polarization parallel ($\parallel$) and perpendicular ($\perp$) to the plane of incidence. Light is incident from air ($n_{inc} = 1$) into a perovskite film with refractive index $n_{mat} = \sqrt{5}$ corresponding to a high frequency dielectric constant of $\epsilon_{\infty} = 5$, which is typical of metal halide perovskites. Light incident at polar angle θ measured from the layer normal transmits into the sample with angle θmat determined by Snell's law, Eq. S30. The amplitude of the components of the electric field of the vector potential are modified by the Fresnel amplitude transmission coefficients $t_{\parallel}$ and $t_{\perp}$ calculated using Eq.S31-S32, respectively. At large incidence angles θ the degree of circular polarization of incident circularly polarized light is reduced due to the fact that the field component perpendicular to the plane of incidence has lower transmission that the field component parallel to the plane of incidence.

B.   Circular dichroism calculation

In the last section we showed how circularly polarized light is modified when it is transmitted at an angle into a planar material. We now calculate the magnitude of absorption, and circular dichroism (CD) for the light interacting with a given j exciton state. We consider light incident on the 2D layer with wave vector $\boldsymbol{k}_{ph}$ at azimuthal angle ϕ measured

from the $\hat{x}$ direction, at polar angle θ measured from the vertical direction $\hat{\boldsymbol{n}}_z$, and has polarization $\hat{\boldsymbol{e}}$ in air. Once transmitted into the medium its magnitude, $\boldsymbol{A}_\pm^m(\theta_{mat}, \phi)$ is given by Eq. S33. The probability of excitation of exciton sub-level j of the ground 2D exciton state with in-plane wave vector $\boldsymbol{K}$ can be described by Fermi's golden rule:

$$\mathcal{W}_{\boldsymbol{K},j} = \frac{2\pi}{\hbar}|\langle\Psi_{\boldsymbol{K},j}|\hat{H}_{\text{int}}|G\rangle|^2 \delta(E_j(\boldsymbol{K}) - \hbar\omega) . \tag{S39}$$

Here, $|G\rangle$ is the crystal ground state, which is represented by $G = \delta(\boldsymbol{r}_e - \boldsymbol{r}_h)^{\text{S6}}$, $\hbar\omega$ is the energy of absorbed photons, and $E_j(\boldsymbol{K})$ is the energy of the jth exciton sub-level.

The light-matter interaction Hamiltonian $\hat{H}_{\text{int}} = -(e/m_0 c)\boldsymbol{A}^m \cdot \hat{\boldsymbol{p}}$ is expressed as usual in terms of the inner product of the dipole operator $\hat{\boldsymbol{p}}$ and the vector potential $\boldsymbol{A}$. To evaluate this matrix element we need the expression for the exciton wave function. The wave functions of these states can be obtained easily in the uncoupled electron hole pair "P" basis , $|u_{j_e=1/2}\rangle|u_{j_h=1/2}\rangle$, $|u_{j_e=1/2}\rangle|u_{j_h=-1/2}\rangle$, $|u_{j_e=-1/2}\rangle|u_{j_h=1/2}\rangle$ and $|u_{j_e=-1/2}\rangle|u_{j_h=-1/2}\rangle$, as,

$$\Psi_{\boldsymbol{K},j}^P(\boldsymbol{R},\boldsymbol{r}) = \frac{\exp(i\boldsymbol{K}\cdot\boldsymbol{R})}{\sqrt{S}} \phi_{1,0}(\boldsymbol{r}) \sum_{j_e=\pm 1/2, j_h=\pm 1/2} C_{j_e,j_h}^j(\boldsymbol{K})|u_{j_e}\rangle|u_{j_h}\rangle \tag{S40}$$

where the coefficients $C_{j_e,j_h}^j(\boldsymbol{K})$ describe the eigenstate of the corresponding matrix. Alternately, having explicitly developed above a description of the exciton fine structure in terms of the $\mathcal{O}$, or D, X, Y, Z basis of exciton states $|D\rangle$, $|X\rangle$, $|Y\rangle$, $|Z\rangle$, whose dipoles are oriented along the X, Y, and Z directions, and the dark D exciton state, we can express the exciton wave function in terms of this basis:

$$\Psi_{\boldsymbol{K},j}^{\mathcal{O}}(\boldsymbol{R},\boldsymbol{r}) = \frac{\exp(i\boldsymbol{K}\cdot\boldsymbol{R})}{\sqrt{S}} \phi_{1,0}(\boldsymbol{r}) \sum_{i=D,X,Y,Z} C_i^j(\boldsymbol{K})|u_i\rangle , \tag{S41}$$

where the coefficients $C_i^j(\boldsymbol{K})$ describe the eigenstate in the basis of exciton states $|u_i\rangle$ running over $|D\rangle$, $|X\rangle$, $|Y\rangle$, $|Z\rangle$.

Either way, evaluating the matrix element in Eq. S39 for the exciton state $\Psi_{\boldsymbol{K},j}$ we find,

$$\langle\Psi_{\boldsymbol{K},j}|\hat{H}_{\text{int}}|G\rangle = \frac{e}{m_0 c}A_0^m\hat{\boldsymbol{e}}\cdot\boldsymbol{P}_j(\boldsymbol{K})\phi_{1,0}(0)\delta_{\boldsymbol{k}_{ph,\perp},\boldsymbol{K}} , \tag{S42}$$

where $\hat{\boldsymbol{e}}$ is the polarization vector inside the layer described in Eq. (S34). The Kronecker delta represents the well-known momentum conservation rule, reflecting conservation of momentum in the 2D layer. The wave vector $\boldsymbol{K}$ of the in-plane exciton created by absorption of a photon must match the in-plane component $\boldsymbol{k}_{ph,\perp} = \boldsymbol{k}_{ph} - \hat{\boldsymbol{n}}_z(\boldsymbol{k}_{ph} \cdot \hat{\boldsymbol{n}}_z)$ of the photon

that was absorbed. The contact term $\phi_{n,0}(0)$ in Eq. S42 is non-zero only for states with $m = 0$. Then, in the uncoupled basis, the transition dipole matrix elements are expressed as,

$$\boldsymbol{P}_j(\boldsymbol{K}) = \sum_{j_e,j_h}[C_{j_e,j_h}^j(\boldsymbol{K})]^*\langle u_{j_e}u_{j_h}|\hat{\boldsymbol{p}}|G\rangle = \sum_{j_e,j_h}[C_{j_e,j_h}^j(\boldsymbol{K})]^*\langle u_{j_e}|\hat{\boldsymbol{p}}\hat{T}|u_{j_h}\rangle \tag{S43}$$

where $\hat{T} = -i\hat{\sigma}_y$ is the time reversal operator written in terms of the Pauli matrix $\hat{\sigma}_y$.[S7] In terms of the D, X, Y, Z basis the exciton transition dipole matrix element are expressed as,

$$\boldsymbol{P}_j(\boldsymbol{K}) = \sum_{i=x,y,z}[C_i^j(\boldsymbol{K})]^*\boldsymbol{P}_i = P_{cv}\sum_{i=x,y,z}[C_i^j(\boldsymbol{K})]^*g_i\hat{\boldsymbol{n}}_i \tag{S44}$$

where $\hat{\boldsymbol{n}}_i$ are the unit vectors along the $\boldsymbol{x}$, $\boldsymbol{y}$ and $\boldsymbol{z}$ directions, $P_{cv} = -i\langle s|\hat{\boldsymbol{p}}_z|z\rangle$ is the Kane momentum matrix element, assumed equal for the $|x\rangle$, $|y\rangle$ and $|z\rangle$ conduction band Bloch states, and g_i is a dimensionless parameter giving the relative magnitude of the transition dipole matrix elements for the $|X\rangle$, $|Y\rangle$ and $|Z\rangle$ exciton basis states. The two representations are related by the basis transformation: $|\Psi^{\mathcal{O}}\rangle = \hat{m}_{F,\mathcal{O}}^{-1}\hat{m}_{P,F}^{-1}|\Psi^P\rangle$, where the unitary transformation matrices are given in Eq. S3 and S6.

In our calculations we prefer the $\mathcal{O}$ basis, and we assume that the x, y and z dipoles have equal relative magnitudes, $g_x = g_y = g_z$. (Expressions for g_i accounting for crystal field effects within a six-band $\boldsymbol{K}\cdot\boldsymbol{P}$ model can be found in Ref. S3). Using Eq. S44 we write the strength of interaction of the exciton state j with the vector potential $\boldsymbol{A}_\pm^m(\theta_{mat}, \phi)$, neglecting common factors, as,

$$I^\pm(j) = |\boldsymbol{A}_\pm^m(\theta_{mat}, \phi)\cdot\boldsymbol{P}_j(\boldsymbol{K})|^2 \tag{S45}$$

It is useful to define a normalized interaction strength for a given set of angles. This should be normalized by the square of the magnitude of the light field, $|A_\pm^m(\theta_{mat}, \phi)|^2$. To normalize the magnitude of the transition dipoles, we note that a given exciton state j has oscillator strength f_j given by[S2,S3],

$$f_j = f_0\tilde{f}_j . \tag{S46}$$

Here, the parameter $f_0 = 2|P_{cv}|^2/(m_0\hbar\omega)$ represents the magnitude of the oscillator strength for a band edge free carrier transition, while $\tilde{f}_j$, introduced in Refs. S2,S3 is a reduced oscillator strength that gives the relative magnitudes of the oscillator strengths among levels within the exciton fine structure. It is proportional to the norm-square of the dipole for the

state: $\tilde{f}_j = |P_j|^2/|P_{cv}|^2 = g_j^2$. Noting that the sum of the reduced oscillator strengths taken over the fine structure levels is a constant, an appropriate normalization is the average of the reduced oscillator strengths taken over the bright exciton basis states X, Y, Z. We therefore define $\tilde{f}_N$ as the as the average,

$$\tilde{f}_N = \frac{g_x^2 + g_y^2 + g_z^2}{3} \tag{S47}$$

Then the average squared norm of the transition dipoles taken over the X, Y, Z bright exciton levels, is $\tilde{f}_N|P_{cv}|^2$. Using this for our dipole normalization we define the normalized interaction strength for exciton state $\boldsymbol{K}$, j, as,

$$I_N^{\pm}(j) = \frac{|\boldsymbol{A}_{\pm}^m(\theta_{mat}, \phi) \cdot \boldsymbol{P}_j(\boldsymbol{K})|^2}{|A_{\pm}^m(\theta_{mat}, \phi)|^2 \tilde{f}_N |P_{cv}|^2} \tag{S48}$$

With this definition we define the circular dichroism for the state j as,

$$\mathcal{P}_j = I_{\text{med}}^{\sigma^+}(j) - I_{\text{med}}^{\sigma^-}(j) \tag{S49}$$

We note that this definition coincides with the degree of polarization for the exciton state in a cubic perovskite with total angular momentum $F_z = \pm 1$ interacting with circularly polarized light propagating in the $\hat{\boldsymbol{z}}$ direction.

C.   Effect of linewidth broadening

The analysis in the last section provides a set of definitions for describing the CD of an individual exciton level. In practice, the exciton transitions are broadened so that the exciton sublevel transitions are often not individually resolvable. We model the effect of linewidth broadening by convolving the absorption spectrum with a Gaussian line-shape function,

$$G(E) = \frac{1}{\sqrt{2\pi}\sigma} e^{-E^2/(2\sigma^2)} \tag{S50}$$

where the full-width at half maximum linewidth is given by $2\sqrt{2\ln 2}\sigma$. We then calculate a normalized absorption spectrum for circularly polarized incident light of $+1$ and -1 helicity as a function of energy, $I_N^{\pm}(E)$, for light incident on the 2D layer with wave vector $\boldsymbol{k}_{ph}$ at polar angle θ and azimuthal angle ϕ. The calculation, made parametrically as a function

of the angles, is,

$$I_N^\pm(E) = \frac{1}{I_{max}} \sum_j I_N^\pm(j) G(E - E_j) \ . \tag{S51}$$

In this expression, the sum is taken over the four exciton sub-levels j for a given $\boldsymbol{K}$, and the normalization factor I_{max} is included to normalize the peak absorption to unity. Then the spectral CD signal is calculated as the difference of the normalized absorption spectra for positive and negative circularly polarized light:

$$P(E) = I_N^+(E) - I_N^-(E) \ . \tag{S52}$$

It should be noted that the spectral CD has a derivative line-shape as shown in the main text, and similar to the phenomenon of magnetic circular dichroism.[S8] It is straightforward to show that in the limit that the level splitting between the $F_{z_B} = \pm 1$ transitions is small compared to the LW, the maximum spectral CD signal occurs at energy $\pm\sigma$ above and below the centroid E_c of the two transitions:

$$\mathrm{CD}_{\max} = |P(E_c \pm \sigma)| \tag{S53}$$

This quantity is calculated and displayed in Fig. 5 of the main text. The definition in Eq. S52 above corresponds to the anisotropy factor defined in Ref. S9. From this quantity, the ellipticity per unit absorbance can be determined at the exciton resonance as $\Theta = P(E) \ln 10/4(180°/\pi)$, or approximately $\Theta = P(E) \times 32.98°$.[S9,S10]

[S1] K. Tanaka, T. Takahashi, T. Kondo, K. Umeda, K. Ema, T. Umebayashi, K. Asai, K. Uchida, and N. Miura, "Electronic and Excitonic Structures of InorganicOrganic Perovskite-Type Quantum-Well Crystal $(C_4H_9NH_3)_2PbBr_4$" *Jpn. J. Appl. Phys., Part 2*, 2005 , **44**, 5923-5932.

[S2] P.C. Sercel, J. L. Lyons, D. Wickramaratne, R. Vaxenburg, N. Bernstein, Al. L. Efros, "Exciton Fine Structure in Perovskite Nanocrystals", *Nano Lett.*, 2019, **19**, 4068- 4077.

[S3] P.C. Sercel, J.L. Lyons, N.Bernstein, Al. L. Efros, "Quasicubic model for metal halide perovskites", *J. Chem. Phys.*, 2019, **151**, 234106.

[S4] T. Kataoka, T. Kondo, R. Ito, S. Kazuhito, K. Uchida, and N. Miura, "Magneto-optical study on excitonic spectra in ($C_6H_13NH_3)_2PbI_4$" *Phys. Rev. B*, 1993, **47**, 2010- 2018.

[S5] E. Hecht, "Optics, Fourth Edition", Addison Wesley, San Francisco, 2002.

[S6] Al. L.Efros, M. Rosen, M. Kuno, M. Nirmal, D.J. Norris, and M. G. Bawendi, " Band-Edge Exciton in Quantum Dots of Semiconductors with a Degenerate Valence Band: Dark and Bright Exciton States." *Phys. Rev B*, 1996, **54**, 4843-4856.

[S7] C. Kittel, "Quantum theory of solids", Wiley, New York, 1987.

[S8] M. Kuno, M. Nirmal, M. G. Bawendi, Al.L. Efros, and M. Rosen, *J. Chem. Phys.*, 1998, **108**, 4242- 4247.

[S9] G. Long, R. Sabatini, M. I. Saidaminov, G. Lakhwani, A. Rasmita, X. Liu, E. H. Sargent, and W. Gao, "Chiral-perovskite optoelectronics", *Nat. Rev.*, 2020, **5**, 423-439.

[S10] P.L. Polavarapu, "Kramers-Kronig Transformation for Optical Rotatory Dispersion Studies", *J. Phys. Chem. A* , 2005, **109**, 7013-7023.